Supporting Information

Electronic structure modification of ultrathin MnFeOOH and integration with Ni₃S₂ as bifunctional electrocatalysts for improved alkaline water splitting

Fu-Min Wang and Si-Fu Tang*

College of Chemistry and Pharmaceutical Sciences, Qingdao Agricultural University,

Changcheng Road 700, Chengyang District, Qingdao 266109, China.

*Corresponding author: tangsf@qau.edu.cn.

Chemicals

NiCl₂·6H₂O and MnCl₂·4H₂O (Tianjin Aopusheng), thiourea from (Tianjin BASF), FeCl₃·6H₂O (Sinopharm), anhydrous ethanol (Yantai Sanhe), nickel foam (NF, 1.0 mm thick, Suzhou Sinero) were all analytical grade and purchased from commercial sources. Before use, the NF was ultrasonic cleaned with 1.0 M HCl, deionized water and anhydrous ethanol to remove the oxide layer and impurities on the surface, and then dried overnight in a vacuum oven at 60 °C.

Instruments

The powder X-ray diffraction (PXRD) measurements of the samples were measured by a polycrystalline X-ray diffractometer (TD-3700) using CuKα radiation. The morphology and elemental mapping of the samples were photographed by the JEOL JSM-IT 500 scanning electron microscope (SEM) equipped with an energy dispersive spectrometer (EDS) system (OXFORD INSTRUMENT, EDAX GENESIS). Inductively coupled plasma-optical emission spectroscopy (ICP-OES) measurements were carried out on PE OPTMA8000DV. X-ray photoelectron spectroscopy (XPS) was recorded on a VG ESCALABMK II spectrometer using an Al Kα (1486.6 eV) photon source, and charging calibrated according to the C 1s peak at 284.8 eV. The thickness of the MnFeOOH nanosheet was measured by atomic force microscopy (AFM) (SHIMADZU SPM-9700HT03040111). The contact angles were measured on Germany KRUSS Cluis DSA25 standard contact angle measuring instrument. The Raman spectra were recorded on a Raman microscopy (DXR2xi, ThermoFisher).

Electrochemical Measurements

All the electrochemical studies were conducted on an electrochemical workstation (CHI 760E) equipped with a three-electrode electrochemical cell in 1.0 M KOH aqueous solution with the prepared catalyst as the working electrode and Hg/HgO as the reference electrode. Platinum plate (1.0×1.0 cm²) and graphite rod (diameter: 0.9 cm) was used as the counter electrode for the OER and HER measurements, respectively. The potentials vs. Hg/HgO were converted to reversible hydrogen electrode (RHE) according to the equation: $E_{\mathrm{RHE}} = E_{\mathrm{Hg/HgO}} + 0.059\mathrm{pH} + 0.098$ V. The linear sweep voltammetry (LSV) curves were measured at a sweep rate of 5 mV s⁻¹ with 75% iR compensation. The Tafel slope was obtained from the LSV polarization

curve based on the Tafel equation. The electrochemical impedance spectroscopy (EIS) was conducted in a frequency range of 100 kHz - 0.01 Hz with an amplitude of 5 mV. Cyclic voltammetry (CV) scans in the appropriate non-Faraday voltage window at different scanning rates were used to determine the double-layer capacitance (C_{dl}) and evaluate the electrochemical active surface area (ECSA). In addition, the electrochemical stability was tested for up to 20 h by chronoamperometry method.
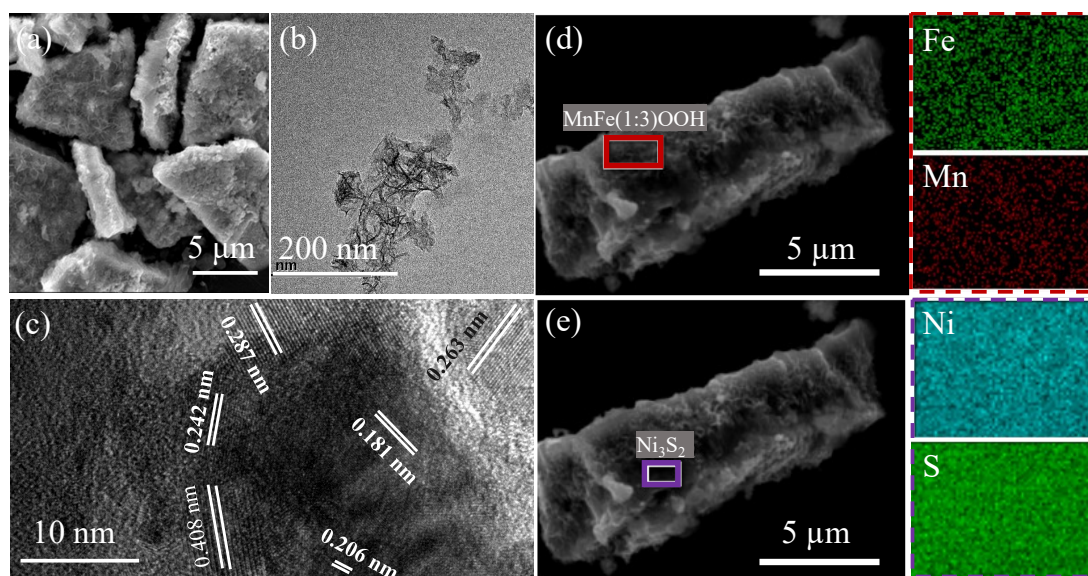

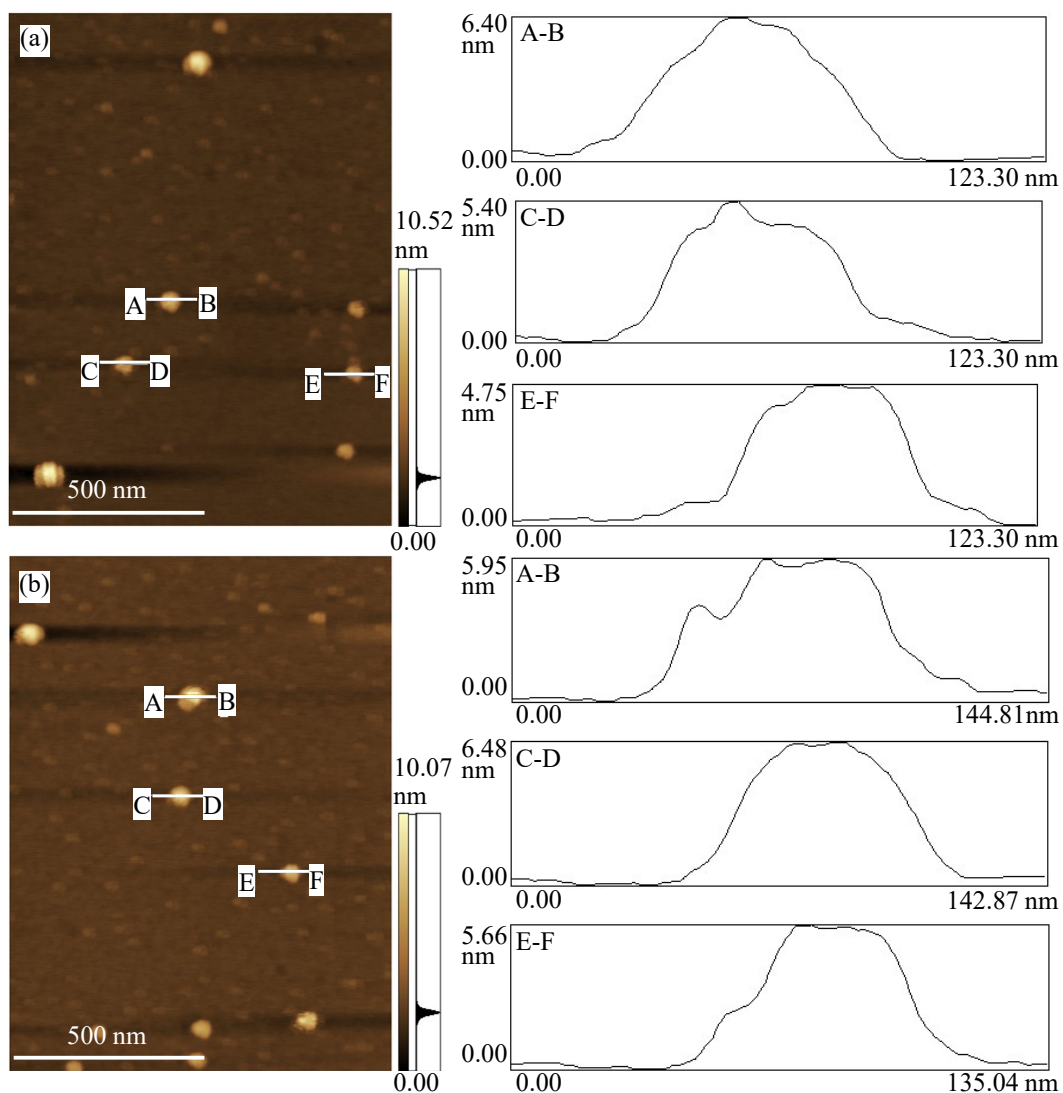Figure S1. SEM (a), TEM (b), HRTEM (c) and EDS (d, e) images of MnFe(1:3)OOH/Ni$_3$S$_2$/NF.

Figure S2. AFM images of MnFe(2:1)OOH/Ni$_3$S$_2$/NF (a) and
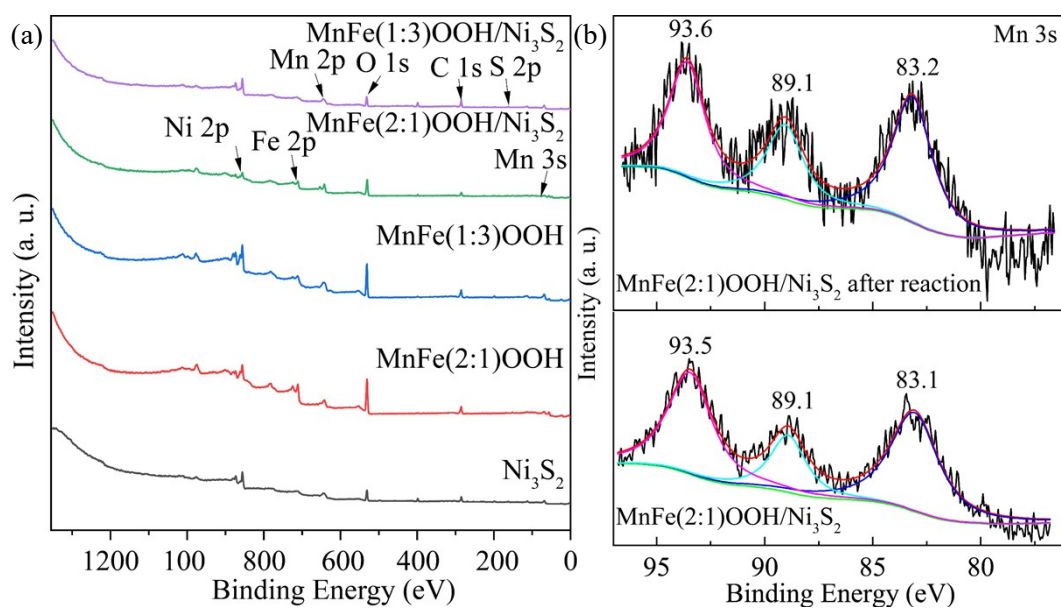MnFe(1:3)OOH/Ni$_3$S$_2$/NF (b).
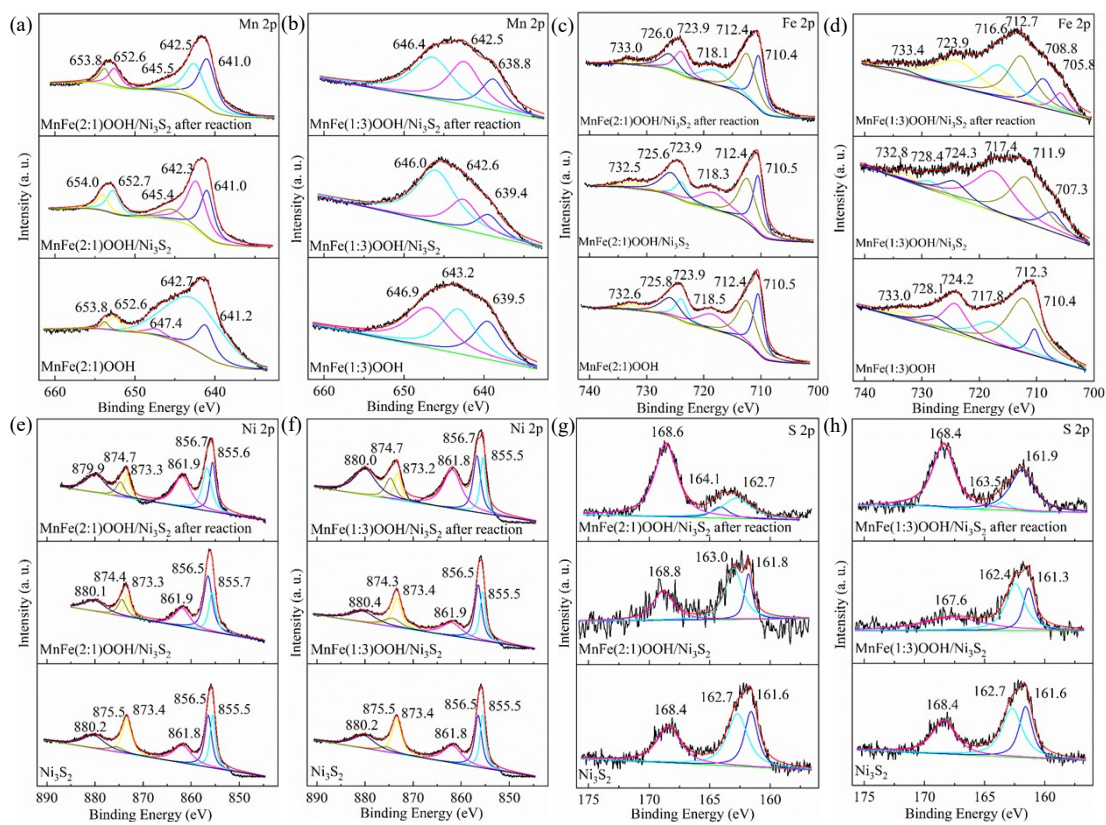

Figure S3. XPS survey and Mn 3s spectra of the catalysts.

Figure S4. XPS Mn 2p (a, b), Fe 2P (c, d), Ni 2p (e, f) and S 2p (g, h) spectra of Ni_3S_2, MnFe(2:1)OOH, MnFe(1:3)OOH, MnFe(2:1)OOH/Ni_3S_2/NF and MnFe(1:3)OOH/Ni_3S_2/NF.
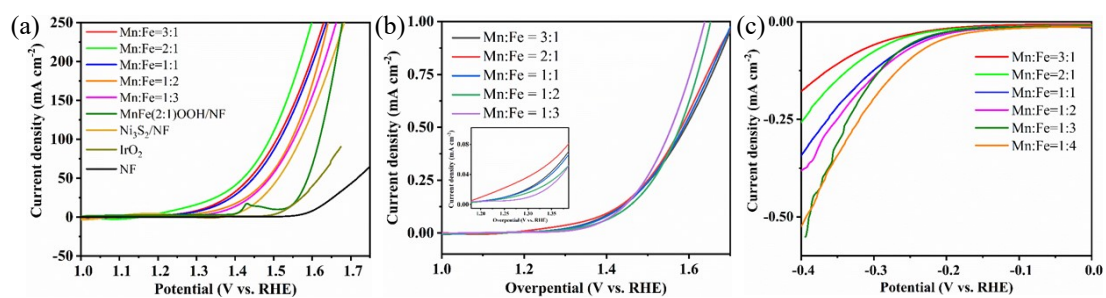

Figure S5. Fitted (a) and ECSA-normalized (b) OER LSV curves (the inset in the enlarged view of the LSV curves in the range of 1.2-1.4 V vs. RHE) and ECSA-normalized HER LSV curves (c) of the catalysts.
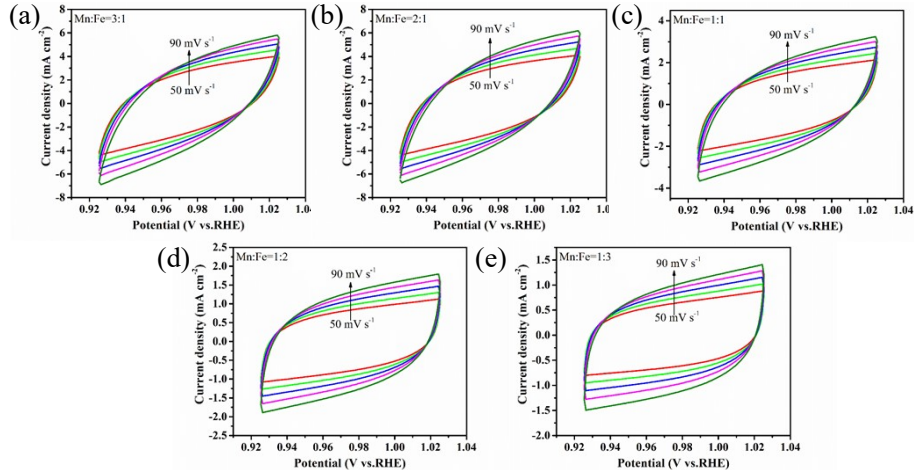
Figure S6. OER CV diagrams of MnFe(3:1)OOH/Ni$_3$S$_2$/NF (a),
MnFe(2:1)OOH/Ni$_3$S$_2$/NF (b), MnFe(1:1)OOH/Ni$_3$S$_2$/NF (c),
MnFe(1:2)OOH/Ni$_3$S$_2$/NF (d), MnFe(1:3)OOH/Ni$_3$S$_2$/NF (e) at different scanning
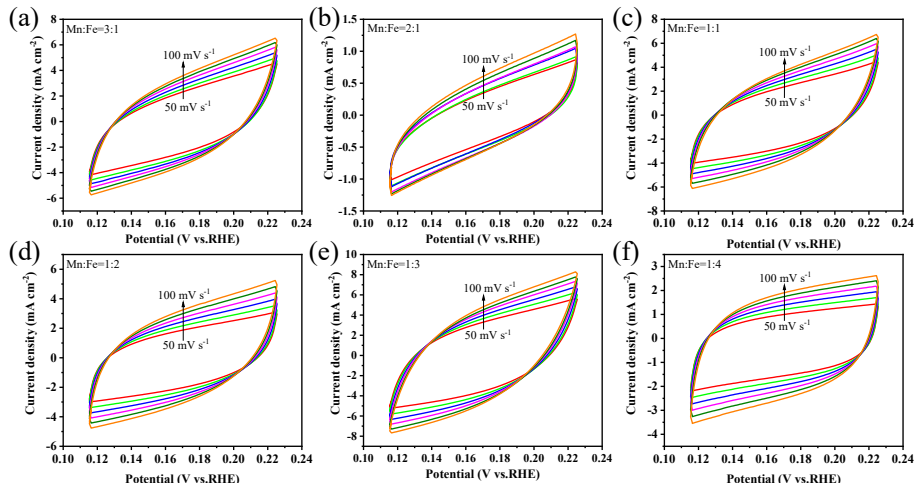rates of 50, 60, 70, 80 and 90 mV s^{-1}.

Figure S7. HER CV diagrams of MnFe(3:1)OOH/Ni$_3$S$_2$/NF (a),
MnFe(2:1)OOH/Ni$_3$S$_2$/NF (b), MnFe(1:1)OOH/Ni$_3$S$_2$/NF (c),
MnFe(1:2)OOH/Ni$_3$S$_2$/NF (d), MnFe(1:3)OOH/Ni$_3$S$_2$/NF (e) and
MnFe(1:4)OOH/Ni$_3$S$_2$/NF (f) at different scanning rates of 50, 60, 70, 80, 90 and 100
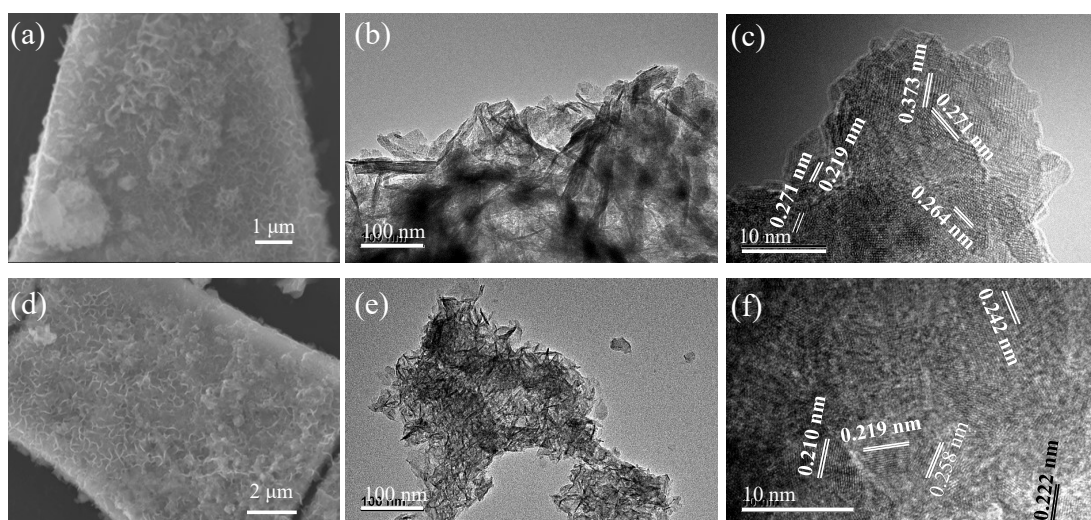mV s^{-1}.

Figure S8. SEM (a), TEM (b) and HRTEM (c) images of MnFe(2:1)OOH/Ni$_3$S$_2$/NF after OER reaction; SEM (d), TEM (e) and HRTEM (f) images of MnFe(1:3)OOH/Ni$_3$S$_2$/NF after HER reaction.
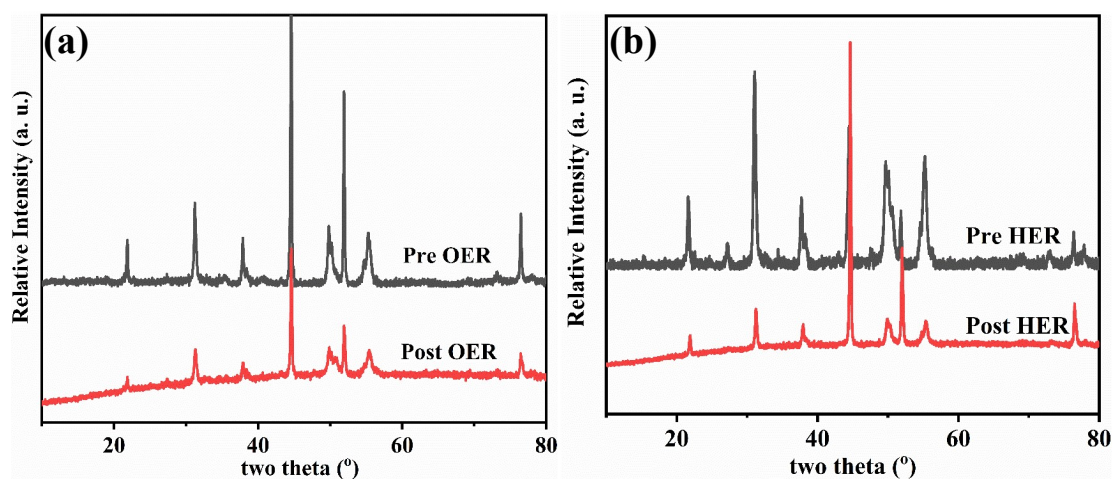

Figure S9. XRD patterns of MnFe(2:1)OOH/Ni$_3$S$_2$/NF (a) and MnFe(1:3)OOH/Ni$_3$S$_2$/NF (b) before and after reaction.

Table S1. OER electrochemistry results of some metal sulfides and their composite catalysts in 1.0 M KOH.

catalysts	η_{10}	η_{50}	η_{100}	reference
Fe(OH)$_3$@Ni$_3$S$_2$/NF-D1–30	173	242	--	1
γ-FeOOH/Ni$_3$S$_2$	--	279	--	2
Ni$_3$S$_2$@MoS$_2$/FeOOH	234	--	--	3
Ni$_3$S$_2$/Co$_3$S$_4$/FeOOH	181	--	--	4
Ni$_3$S$_2$/MoS$_2$/FeOOH	--	--	219	5
δ-FeOOH/Ni$_3$S$_2$	187	--	--	6
Ni(Fe)OOH/Ni(Fe)S$_x$	227	--	--	7
Fe11.8%-Ni$_3$S$_2$/NF	--	--	253	8

NiFe–S-13@CNFs	270	--	--	9
MoS_2/Ni_3S_2	185	--	--	10
Mo-W-S-2@Ni_3S_2	285	--	--	11
V-Ni_3S_2@NiO	170	--	310	12
Ni_3S_2-$CoMoS_x$	234	--	--	13
Ni_3S_2@$FeNi_2S_4$@NF	235	--	--	14
FeS/Ni_3S_2@NF	192	--	--	15
FeOOH/Ga-Ni_3S_2	--	235	274	16
MnFe(2:1)OOH/Ni_3S_2/NF	--	--	268.4	This work

Table S2. HER electrochemistry results of some metal sulfides and their composite catalysts in 1.0 M KOH.

catalysts	η_{10}	η_{50}	η_{100}	reference
γ-FeOOH/Ni_3S_2	92	--	--	2
Ni_3S_2@MoS_2/FeOOH	95	--	--	3
Ni_3S_2/Co_3S_4/FeOOH	158	--	--	4
Ni_3S_2/MoS_2/FeOOH	76	--	--	5
δ-FeOOH/Ni_3S_2	106	--	--	6
MoS_2/Ni_3S_2	99	--	--	10
Mo-W-S-2@Ni_3S_2	98	--	--	11
V-Ni_3S_2@NiO	112	--	239	12
Ni_3S_2-$CoMoSx$	90	--	--	13
Ni_3S_2@$FeNi_2S_4$@NF	83	--	--	14
FeS/Ni_3S_2@NF	130	--	--	15
MnFe(1:3)OOH/Ni_3S_2/NF	94.6	257.6	294.6	This work

Table S3. Cell voltages of some Ni_3S_2, FeOOH, MnOOH and their composite catalysts in 1.0 M KOH.

catalysts	Cell voltage at 10 mA/cm^2	reference
γ-FeOOH/Ni_3S_2	1.66	2
Ni_3S_2@MoS_2/FeOOH	1.57	3
Ni_3S_2/MoS_2/FeOOH	1.58	5
δ-FeOOH/Ni_3S_2	1.53	6
MoS_2/Ni_3S_2/NF	1.50	10
Mo-W-S-2@Ni_3S_2	1.62	11
V-Ni_3S_2@NiO	1.52	12
Ni_3S_2-$CoMoS_x$	1.52	13
NiO-Ni_3S_2/NF	1.57	17
$Ni_xCo_{3-x}S_4$/Ni_3S_2/NF	1.53	18
NiFe-LDHs @γ-MnOOH	1.69	19
MnFe(2:1)OOH/Ni_3S_2/NF‖MnFe(1:3)OOH/Ni_3S_2/NF	1.60	This work

Reference:

1   H. Yan, R. Deng, C. Wang, H. Yao, S. Guo, R. Liu, S. Ma. *Electrochimica Acta*, 2022, **427**, 140889.

2   Y. Liu, M. Ding, Y. Tian, G. Zhao, J. Huang, X. Xu. *J. Colloid Interface Sci.*, 2023, **639**, 24–32

3   M. Zheng, K. Guo, W.-J. Jiang, T. Tang, X. Wang, P. Zhou, J. Du, Y. Zhao, C. Xu, J.-S. Hu. *Appl. Catal. B: Environ.*, 2019, **244**, 1004–1012.

4   C. Fan, X. Shen, J. Cheng, L. Lang, G. Liu, Z. Ji, G. Zhu. *Colloid Surface A*, 2021, **631**, 127689.

5   C. Fan, X. Yue, X. Shen, J. Cheng, W. Ke, Z. Ji, A. Yuan, G. Zhu. *ChemElectroChem,* 2021, **8**, 665-674.

6   X. Ji, C. Cheng, Z. Zang, L. Li, X. Li, Y. Cheng, X. Yang, X. Yu, Z. Lu, X. Zhang, H. Liu. *J. Mater. Chem. A*, 2020, **8**, 21199–21207.

7   M. Chen, W. Li, Y. Lu, P. Qi, H. Wu, G. Liu, Y. Zhao, Y. Tang. *J. Mater. Chem. A*, 2023, **11**, 4608–4618.

8   N. Cheng, Q. Liu, A. M. Asiri, W. Xing, X. Sun. *J. Mater. Chem. A*, 2015, **3**, 23207–23212.

9   Y. Li, W. Ma, J. Wang, Q. Zhong. *J. Mater. Chem. A*, 2022, **10**, 24388–24397.

10 F. Li, D. Zhang, R.-C. Xu, W.-F. Fu, X.-J. Lv. *ACS Appl. Energy Mater.* 2018, **1**, 3929−3936.

11 M. Zheng, J. Du, B. Hou, C.-L. Xu. *ACS Appl. Mater. Interfaces* 2017, **9**, 26066−26076.

12 Q. Liu, J. Huang, L. Cao, K. Kajiyoshi, K. Li, Y. Feng, C. Fu, L. Kou, L. Feng. *ACS Sustainable Chem. Eng.* 2020, **8**, 6222−6233.

13 L. Zhao, H. Ge, G. Zhang, F. Wang, G. Li. *Electrochim. Acta*, 2021, **387**, 138538.

14 Y. Yang, H. Meng, C. Kong, S. Yan, W. Ma, H. Zhu, F. Ma, C. Wang, Z. Hu. *J. Colloid Interface Sci.*, 2021, **599**, 300–312.

15 H. Li, S. Yang, W. Wei, M. Zhang, Z. Jiang, Z. Yan, J. Xie. *J. Colloid Interface Sci.*, 2022, **608**, 536–548.

16 R. Wang, Y. Yang, X. Xu, S. Chen, A. Trukhanov, R. Wang, L. Shao, X. Lu, H. Pan, Z. Sun. *Inorg. Chem. Front.*, 2023, **10**, 1348–1356.

17 L. Peng, J. Shen, X. Zheng, R. Xiang, M. Deng, Z. Mao, Z. Feng, L. Zhang, L. Li, Z. Wei. *J. Catal.*, 2019, **369**, 345–351.

18 Y. Wu, Y. Liu, G.-D. Li, X. Zou, X. Lian, D. Wang, L. Sun, T. Asefa, X. Zou. *Nano Energy*, 2017, **35**, 161–170.

19 S.-B. Wang, Y.-S. Xia, Z.-F. Xin, L.-X. Xu. *Catal. Commun.*, 2023, **173**, 106564.